MA8109 Project
Using SDEs to model diffusion with reflecting boundaries
Student nr. 659863

1 Introduction

In applied meteorology and oceanography, it is common to model advection-diffusion problems with so-called "Lagrangian particle methods". This amounts to solving an SDE for an ensemble of trajectories, in such a way that the distribution of trajectories evolves in a manner consistent with the advection-diffusion equation. Throughout this report, the term "numerical particle", or just "particle", will be used to refer to a single realisation of a solution of an SDE.

There are both advantages and disadvantages to using Lagrangian particle methods, compared to direct numerical solution of the advection-diffusion equation (so-called Eulerian methods). Advantages include explicit conservation of mass, favourable numerical properties for advection-dominated problems, and the ability to give each particle different properties. The latter point is of particular relevance when modelling a substance with a wide range of settling or rising velocities, *e.g.*, mineral grains or oil droplets. In these cases, the settling or rising velocity can vary by several orders of magnitude, due to the wide size distributions involved. In a Lagrangian model, each numerical particle can have its own settling or rising velocity, facilitating a good representation of the true distribution of velocities. In the Eulerian approach, one would have to solve one advection-diffusion equation for each velocity, making it computationally demanding to accurately represent a wide distribution.

Disadvantages to Lagrangian methods include the need to use very large numbers of particles if one needs to resolve dilute concentrations, and the fact that SDE methods and their theory is somewhat inaccessible compared to PDE methods. For an overview of Lagrangian oceanography, see, *e.g.*, van Sebille, et al. (2018), and for a concrete example of an application to oil droplets see, *e.g.*, Nordam, et al. (2019).

1.1 This project

In this project, we will consider a one-dimensional diffusion problem on a finite domain, with no-flux boundary conditions. The diffusion will be simulated by an SDE, which will be derived from the diffusion equation, and solved by the Euler-Maruyama method. The aim of the project is to implement and compare two different schemes for enforcing the no-flux boundary conditions. A numerical investigation of the order of weak convergence will be made for both schemes.

2 Theory

The one-dimensional diffusion equation, for a concentration $C(z,t)$, with variable diffusivity $K(z)$, is

$$\frac{\partial C}{\partial t} = \frac{\partial}{\partial z}\left(K\frac{\partial C}{\partial z}\right). \tag{1}$$

The link from concentration to a probability distribution, p, of particle positions, is found by normalising C:

$$p(z,t) = \frac{C(z,t)}{\int_0^L C(z,t)\,\mathrm{d}z}. \tag{2}$$

2.1 An SDE model for the diffusion equation

Consider an Itô diffusion process described by the SDE

$$\mathrm{d}z = a(z)\,\mathrm{d}t + b(z)\,\mathrm{d}W_t, \tag{3}$$

where a and b are called respectively the drift and diffusion coefficients. Assume that $a(z)$ and $b(z)$ are "moderately smooth functions" (Kloeden and Platen, 1992, p. 37) (for more details see, *e.g.*, Gihman and Skorohod (1972, pp. 96–102)). For this diffusion process, the Fokker-Planck equation for evolution of the

transition probability density, $p(z, t \,|\, z_0, t_0)$, from an initial position z_0 at time t_0, to a position z at a later time t, is (Kloeden and Platen, 1992, p. 37):

$$\frac{\partial p}{\partial t} = \frac{1}{2}\frac{\partial^2}{\partial z^2}\big(b^2 p\big) - \frac{\partial}{\partial z}\big(ap\big), \tag{4}$$

where we have dropped the arguments to a, b and p for brevity. Rewriting a bit, we get

$$\frac{\partial p}{\partial t} = \frac{1}{2}\frac{\partial}{\partial z}\left(b^2\frac{\partial p}{\partial z}\right) - \frac{\partial}{\partial z}\left[\left(a - \frac{1}{2}\frac{\partial b^2}{\partial z}\right)p\right]. \tag{5}$$

We then compare Eq. (5) to the diffusion equation (Eq. (1)). By matching terms, and using that C is proportional to p, we find that $K = b^2/2 \Rightarrow b = \sqrt{2K}$, and $a = \partial_z K$. Hence, the SDE whose probability density is described by the diffusion equation is

$$\mathrm{d}z = K'(z)\,\mathrm{d}t + \sqrt{2K(z)}\,\mathrm{d}W_t, \tag{6}$$

where $K'(z) = \partial_z K\big|_z$.

2.2 Numerical solution of SDEs

To integrate Eq. (6), we introduce a discrete time, $t_n = t_0 + n\Delta t$, and use the Euler-Maruyama method (Maruyama, 1955; Kloeden and Platen, 1992, p. 305), which yields

$$z_{n+1} = z_n + K'(z_n)\Delta t + \sqrt{2K(z_n)}\Delta W_n, \tag{7}$$

where ΔW_n are iid Gaussian random numbers with expectation value $\langle \Delta W_n \rangle = 0$ and variance $\langle \Delta W_n^2 \rangle = \Delta t$.

2.3 Reflecting boundary

As mentioned in the introduction, we consider a finite domain, $z \in [0, L]$, with reflecting (no-flux) boundary conditions. We now investigate two different approaches to implementing the reflecting boundary.

2.3.1 Simple reflection

A simple implementation of reflecting boundaries is to take steps with the Euler-Maruyama method, and after each step reflecting any trajectories back into the domain, if they end up outside:

$$z_n \to \begin{cases} -z_n & \text{if} \quad z_n < 0, \\ 2L - z_n & \text{if} \quad z_n > L, \\ z_n & \text{otherwise.} \end{cases} \tag{8}$$

While it is theoretically possible for a solution to be reflected from outside one boundary, to a point beyond the other boundary, we will assume that Δt is small enough to make this process negligible.

2.3.2 Lépingle's scheme

An alternative scheme for SDEs with reflecting boundary conditions is described by Lépingle (1993, 1995). Lépingle's scheme is motivated by the observation that even if a trajectory is inside the domain at both times t_n and t_{n+1}, it has some probability of having been outside in between. This is illustrated in Fig. 1. The idea is then that instead of solving an SDE

$$\mathrm{d}z = a\,\mathrm{d}t + b\,\mathrm{d}W_t, \tag{9}$$

and enforcing the reflecting boundary in a *post hoc* manner as above, we solve the modified equation

$$\mathrm{d}z = a\,\mathrm{d}t + b\,\mathrm{d}W_t + \mathrm{d}K_t. \tag{10}$$

Here, K_t is in some sense "the minimal process" that forces $z(t)$ to remain inside our domain *at all times* (Lépingle, 1995). In order to obtain a discrete version of K_t suited for numerical simulation, we start with the following result:

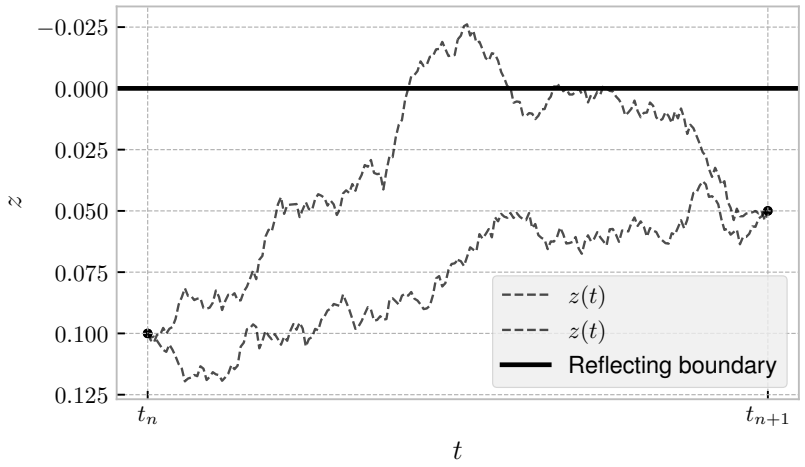

Figure 1: Illustration of two possible trajectories of $z(t)$, between the two points (z_n, t_n), and (t_{n+1}, z_{n+1}). Even if the solution is inside the domain both at t_n and t_{n+1}, it may have been outside in between.

Theorem 1 (adapted from Lépingle (1993, 1995)): Let a and b be real numbers, let W_t be a Brownian motion, and $\Delta t = t_{n+1} - t_n$. Then, let

$$S_{t_n} = \sup_{t_n \le t \le t_{n+1}} \big[a(t - t_n) + b(W_t - W_{t_n})\big]. \tag{11}$$

Let U_n be a Gaussian random variable, with zero mean, $\langle U_n \rangle = 0$, and variance $\langle U_n^2 \rangle = \Delta t$, and let V_n be an exponential random variable with parameter $(2\Delta t)^{-1}$, independent of U_n. Finally, define a new random variable, Y_n, given by

$$Y_n = \frac{1}{2}\left[a\Delta t + bU_n + \sqrt{a^2 V_n + (a\Delta t + bU_n)^2}\right]. \tag{12}$$

Then, the vectors $(\Delta W_n, S_{t_n})$ and (U_n, Y_n) have the same distribution.

The proof of this theorem is given (in French) in Lépingle (1993). The result has been adapted to one dimension, and to match the notation otherwise used in this report.

For numerical implementation of a reflecting boundary at $z = 0$, Lépingle (1995) suggests the following modification of the Euler-Maruyama scheme:

$$z_{n+1} = z_n + a(z_n)\Delta t + b(z_n)\,\Delta W_n + \max(0, A_n - z_n), \tag{13a}$$

where

$$A_n = \sup_{t_n \le t \le t_{n+1}} \big[-a(z_n)\,(t - t_n) - b(z_n)\,(W_t - W_{t_n})\big]. \tag{13b}$$

From Theorem 1, we see that we can use Eq. (12) to simulate the random variable A_n, with the desired distribution. In particular, we use $U_n = \Delta W_n$ in Eq. (12), which guarantees that $z_{n+1} \ge 0$ (see Appendix A). The same scheme is also readily adapted to the reflecting boundary at $z = L$.

2.4 The well-mixed condition

The well-mixed condition (WMC), described by Thomson (1987), is a commonly used criterion to test practical implementations of Lagrangian particle models. It essentially says that in a diffusion problem ($K(z) > 0 \;\forall\; z$), an initially well-mixed (*i.e.*, evenly distributed) tracer should remain well mixed for all

times (provided that the tracer cannot escape through any boundaries). That this must be so is easily seen from the diffusion equation (Eq. (1)). If $\partial_z C = 0$ everywhere, including at any boundaries, then we also have $\partial_t C = 0$, and the concentration must remain unchanged. Note that satisfying the WMC is a necessary, but not sufficient, condition for a particle model to be consistent with the diffusion equation.

3 Numerical results

To numerically investigate the two reflection schemes described above, we will make use of the WMC. We will first simulate an initially well-mixed tracer, in constant and variable diffusivity, and look directly at the concentration, $C(z,t)$, averaged over time. We will then consider the expectation values of the particle positions, $\langle z_n \rangle$, and investigate the order of weak convergence for both schemes.

3.1 Diffusivity

We consider a variable diffusivity, $K(z)$, representative for wind-mixing near the ocean surface (Visser, 1997):

$$K(z) = K_0 + zK_1 \mathrm{e}^{-z\alpha}, \tag{14a}$$

$$K_0 = 2 \times 10^{-4}\ \mathrm{m}^2/\mathrm{s}, \qquad K_1 = 2 \times 10^{-3}\ \mathrm{m/s}, \qquad \alpha = 0.5\ \mathrm{m}^{-1}. \tag{14b}$$

where z is depth (positive downwards), and K_0, K_1, α are constants. We also consider a constant diffusivity,

$$K(z) = K_0, \qquad K_0 = 2 \times 10^{-3}\ \mathrm{m}^2/\mathrm{s}. \tag{15}$$

The two diffusivities are shown in the left panel of Fig. 2.

3.2 Well-mixed condition – Concentration

In order to investigate if the WMC is satisfied, $N_p = 1\,000\,000$ initial positions were selected from a uniform random distribution between 0 and $L = 2$ m. Eq. (6) was integrated in time for a duration $T = 6$ hours, for each initial condition, using both reflection schemes, and two different timesteps, $\Delta t = 10\,\mathrm{s}$ and $\Delta t = 50\,\mathrm{s}$. At each step in the simulations, the density of particles was calculated by bin counts (histogram) in 200 bins. Finally, the density was averaged in time over the duration of the simulation, to reduce random noise.

For the constant diffusivity (Eq. (15), results shown in the middle panel of Fig. 2), we observe that the density of particles remains constant (up to random fluctuations), for both schemes and both values of the timestep (the middle panel of Fig. 2 contains the same four lines as the right panel, but they are hard to discern as they are virtually identical). This is consistent with what we expect from the WMC.

For variable diffusivity (Eqs. (14), results shown in the right panel of Fig. 2), we observe that there is a deviation from constant density, mainly at the boundary at $z = 0$. The deviation is larger for $\Delta t = 50$ s than for $\Delta t = 10$ s, and larger for the Lépingle scheme than for Euler-Maruyama with simple reflection. We note that there is no corresponding deviation at the boundary at $z = L$. It seems likely that this is because $K(z)$ approaches a constant at this boundary (see left panel of Fig. 2).

3.3 Well-mixed condition – Weak convergence

In order to investigate the order of weak convergence, we run simulations like those presented in the previous subsection, for a range of different timesteps, Δt. We will only consider the case with variable diffusivity. We select $N_p = 100\,000\,000$ initial positions, from a uniform distribution between 0 and $L = 2$ m. Hence, we have $\langle z_0 \rangle = L/2$, and by the WMC we should have $\langle z_n \rangle = L/2$ for all t_n. We can use this to investigate the weak convergence by considering the error in the expectation value

$$E(\Delta t) = |\langle z_n(\Delta t) \rangle - L/2|, \tag{16}$$

for different timesteps, Δt. The results are shown in Fig. 3, where in each case $\langle z_n \rangle$ has been averaged in time over the last 5 hours of a 6 hour simulation. The order of convergence has been inferred by linear fit

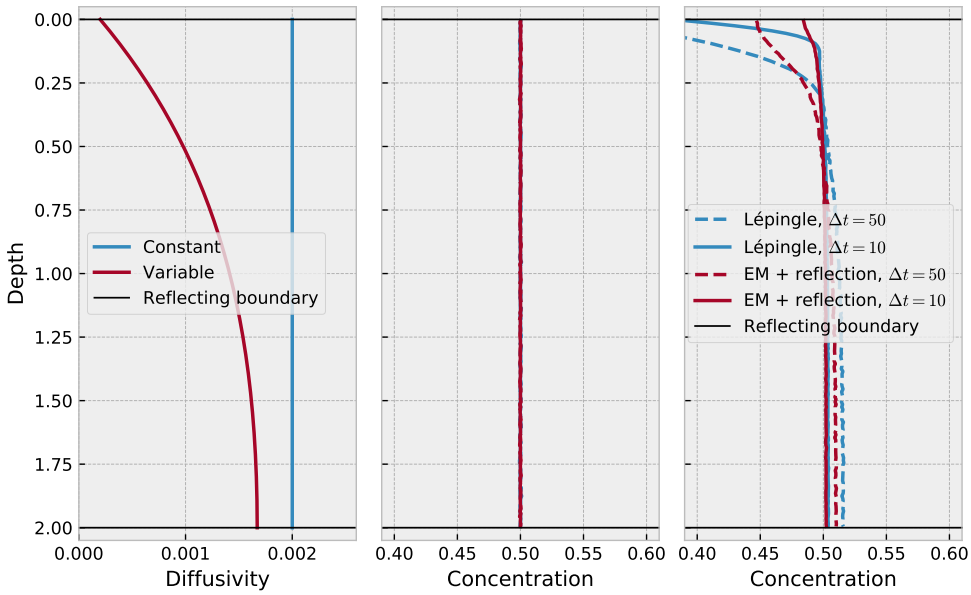

Figure 2: Left panel: Diffusivity as a function of z. Middle panel: Density of $N_p = 1\,000\,000$ initially evenly distributed particles, averaged over a simulation period of 6 hours, for constant diffusivity. Right panel: The same for variable diffusivity. The legend in the right panel also applies to the middle panel.

of the logarithm of the error to the logarithm of the timestep. As the error is expected to flatten out at large timesteps, and as the error at small timesteps is dominated by random noise due to finite number of samples, only the results for intermediate timesteps (filled points in Fig. 3) were used to perform the fit.

From the results obtained here, it appears that Euler-Maruyama with simple reflection has weak order of convergence 1 (the value found was 0.995, though this changes a little if more or fewer points are included in the linear fit). The Lépingle scheme, on the other hand, appears to have a slightly lower weak order of convergence, of around 0.92.

4 Discussion and Conclusion

We have derived an SDE, whose Fokker-Plack equation is the diffusion equation. We have described two different approaches to enforcing reflecting boundary conditions: Simple reflection, and the Lépingle scheme. Numerical simulations were first done to see if the schemes satisfy the so-called well-mixed condition. From looking at the distributions shown in the right panel of Fig. 2, we see that in the case of variable diffusivity, both schemes yield particle distributions that deviate from the WMC. In particular, there is a reduced density of particles near the boundary at $z = 0$, and a matching increase in particle density throughout the rest of the domain. We note that the deviation occurs only at $z = 0$, and not at $z = L$. A likely explanation seems to be that this is related to the fact that $K'(L) = 0$, while $K'(0) > 0$ (see left panel of Fig. 2).

We also found that the Lépingle scheme has a lower weak order of convergence (approximately 0.92), compared to the Euler-Maruyama scheme with simple reflection (approximately 1.0). For the problem and the timesteps considered here, the error in $\langle z_n \rangle$ was approximately 2-3 times larger for the Lépingle scheme. To understand why this is so, we look at the right panel of Fig. 2 and see that the Euler-Maruyama scheme with simple reflection gives a too low density of particles near the boundary at $z = 0$ (for the case considered here). The description of the Lépingle scheme in Section 2.3.2 suggests that the net effect of this scheme is to "push" the reflected particles even further away from the boundary, compared to the simple reflection scheme (see Appendix C). From the right panel of Fig. 2, we see that the Lépingle scheme does indeed give even lower particle density near the boundary at $z = 0$, compared to Euler-Maruyama with simple reflection.

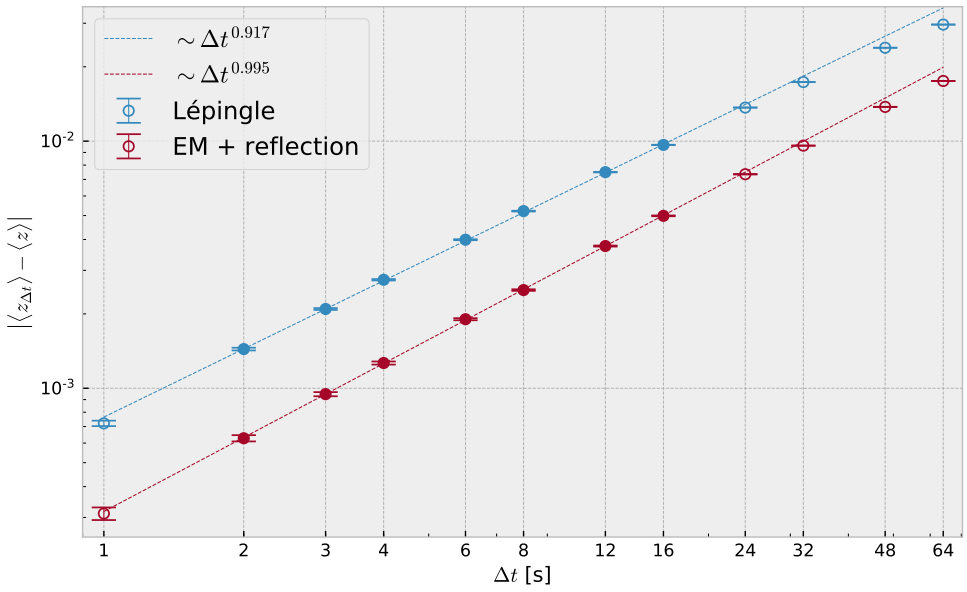

Figure 3: Error in expectation value (Eq. (16)) for the two different reflection schemes, for variable diffusivity (Eqs. (14)), at different timesteps. The slopes of the dashed lines have been obtained by linear fit of the logarithm of the error to the logarithm of the timestep. Only the filled datapoints were used for the regression analysis. The errorbars show the interval $[E(\Delta t)-\sigma_N, E(\Delta t)+\sigma_N]$, where $\sigma_N = L/\sqrt{12N}$ (see Appendix B).

We conclude that while both schemes give correct results for constant diffusivity, and appear to converge to the correct result for variable diffusivity, the Euler-Maruyama scheme with simple reflection seems best suited to this application. In particular, it is simpler to implement, gives a smaller error for the timesteps considered, and appears to have a higher weak order of convergence.

References

P. Billingsley. *Probability and measure*. John Wiley & Sons, New York Chichester Brisbane Toronto, 1979.

I.I. Gihman and A.V. Skorohod. *Stochastic differential equations*. Springer-Verlag, Berlin Heidelberg New York, 1972.

P.E. Kloeden and E. Platen. *Numerical solution of stochastic differential equations*. Springer-Verlag, Berlin Heidelberg New York, 1992.

D. Lépingle. Un schéma d'Euler pour équations différentielles stochastiques réfléchies. *Comptes rendus de l'Académie des sciences. Série 1, Mathématique*, 316(6):601–605, 1993.

D. Lépingle. Euler scheme for reflected stochastic differential equations. *Mathematics and Computers in Simulation*, 38(1-3):119–126, 1995.

G. Maruyama. Continuous Markov processes and stochastic equations. *Rendiconti del Circolo Matematico di Palermo*, 4(1):48, 1955.

T. Nordam, et al. On the use of random walk schemes in oil spill modelling. *Marine pollution bulletin*, 146: 631–638, 2019.

D.J. Thomson. Criteria for the selection of stochastic models of particle trajectories in turbulent flows. *Journal of Fluid Mechanics*, 180:529–556, 1987.

E. van Sebille, et al. Lagrangian ocean analysis: Fundamentals and practices. *Ocean Modelling*, 121:49–75, 2018.

A.W. Visser. Using random walk models to simulate the vertical distribution of particles in a turbulent water column. *Marine Ecology Progress Series*, 158:275–281, 1997.

Appendix

A Check that the Lépingle scheme enforces no-flux boundary

Here, we check that the Lépingle scheme for a reflecting boundary at $z = 0$ does indeed enforce $z_n \geq 0$, for all t_n. First, note that for the exponentially distributed variable in Eq. (12), we have $V_n \geq 0$. Using $U_n = \Delta W_n$, as described by Lépingle (1995), and setting $V_n = 0$, we obtain

$$z_{n+1} = z_n + a(z_n)\Delta t + b(z_n)\,\Delta W_n + \max(0, A_n - z_n), \tag{17a}$$

$$A_n = -a(z_n)\Delta t - b(z_n)\Delta W_n, \tag{17b}$$

which yields

$$z_{n+1} = \begin{cases} z_n + a(z_n)\Delta t + b(z_n)\Delta W_n & \text{if} \quad \big(z_n + a(z_n)\Delta t + b(z_n)\Delta W_n\big) > 0, \\ 0 & \text{otherwise.} \end{cases} \tag{18}$$

Hence, we see that even with $V_n = 0$ (which is the smallest possible value of V_n), we have $z_{n+1} \geq 0$, and the value of A_n is strictly increasing with V_n (see Eq. (12)).

A similar analysis applies to the reflecting boundary at $z = L$.

B Quantify sample error in convergence plot

Each datapoint in Fig. 3 is given by $|\mu_N(\Delta t) - \mu|$, where $\mu = L/2$ is the correct expectation value, and $\mu_N(\Delta t)$ is the sample mean, $\langle z_n \rangle$, obtained from N samples, with a timestep Δt. The sample mean is an approximation of $\mu(\Delta t)$, which is the true expectation value of the distribution of the numerical solutions, obtained with timestep Δt. By the strong law of large numbers, we have that $\mu_N(\Delta t) \to \mu(\Delta t)$ as $N \to \infty$, almost surely (Billingsley, 1979, p. 85).

Note that while the *correct* expectation value is $L/2$ by the WMC, $\mu(\Delta t)$ is in general different from $L/2$ for non-zero timesteps, due to the systematic error of the numerical scheme. The origin of this systematic error in expectation value is the deviation from the WMC which can be observed in the right panel of Fig. 2.

When investigating the weak order of convergence, we would ideally like to know how $|\mu(\Delta t) - \mu|$ scales with the timestep, but for a numerical investigation we are limited to instead consider $|\mu_N(\Delta t) - \mu|$. We then have to make sure that N is sufficiently large, such that the error we observe is indeed due to the timestep, and not dominated by random sampling error. To check this, we can use a version of the Central Limit Theorem to estimate the sampling error.

According to the Lindeberg-Lévy Theorem (Billingsley, 1979, p. 308), we have

$$\frac{\sqrt{N}}{\sigma(\Delta t)} |\mu_N(\Delta t) - \mu(\Delta t)| \sim \mathcal{N}(0, 1), \tag{19}$$

where $\sigma^2(\Delta t)$ is the true variance of the distribution of numerical solutions obtained with timestep Δt. This true variance is not known, but we know (see Fig. 2, right panel) that for reasonably small timesteps Δt the distribution is close to a uniform distribution between 0 and L. Hence we use the approximate value $\sigma^2(\Delta t) \approx L^2/12$, for all timesteps Δt.

Regarding the number of samples, N, we calculated $N_p = 100\,000\,000$ numerical solutions (with different initial conditions) for each value of the timestep. Furthermore, each simulation was run for a duration $T = 6$ hours. For each timestep, the time-development of $\mu_N(\Delta t)$ was investigated. In particular, the auto-correlation in time was plotted (not shown here), and it was found that the de-correlation time was approximately half an hour for all timesteps. Hence, we assume that taking the average over the last 5 hours of a 6-hour simulation constitutes 10 independent samples, and we use $N = 10N_p$. For the numerical values used to obtain Fig. 3, we find that the standard deviation in the sample error, $|\mu_N(\Delta t) - \mu(\Delta t)|$, is given by

$$\sigma_N = \frac{L}{\sqrt{12N}} = \frac{1}{\sqrt{30}} \cdot 10^{-4} \text{ m} \approx 1.8 \cdot 10^{-5} \text{ m}. \tag{20}$$

The error bars in Fig. 3 indicate in each case $\pm\sigma_N$. While some approximations have been made here, the relatively small standard deviation suggest that the scaling of the error in Fig. 3 is indeed due to the timestep, and not random sampling errors caused by too few samples.

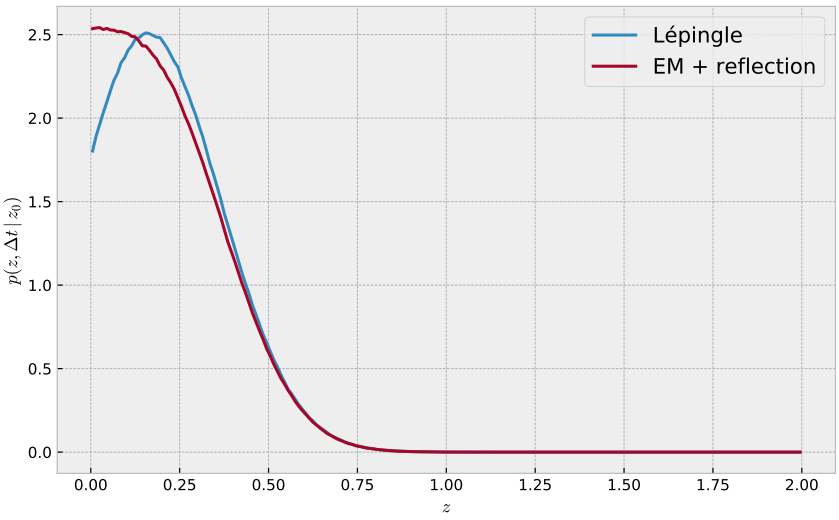

Figure 4: Distribution of $N_p = 100\,000\,000$ particles, all starting at $z_0 = 0.1\,\mathrm{m}$, after one step of duration $\Delta t = 50\,\mathrm{s}$ for both schemes.

C Comparison of the distribution of reflected particles

To illustrate the behaviour of the Lépingle scheme, a simple numerical test was conducted. $N_p = 10\,000\,000$ particles were initially placed at $z_0 = 0.1\,\mathrm{m}$. Then, one step of duration $\Delta t = 50\,\mathrm{s}$ was made with both schemes, using the variable diffusivity given by Eqs. (14). The resulting distributions of particles are then an approximation of $p(z, \Delta t \mid z_0 = 0.1\,\mathrm{m})$ for each scheme. The distributions are shown in Fig. 4. We observe that the net effect of the Lépingle scheme is that particles close to the boundary at $z = 0$ are "pushed" a little further away, compared to Euler-Maruyama with simple reflection.